bioRxiv preprint doi: https://doi.org/10.1101/432302; this version posted October 1, 2018. The copyright holder for this preprint (which was not certified by peer review) is the author/funder, who has granted bioRxiv a license to display the preprint in perpetuity. It is made available under aCC-BY 4.0 International license.

Stage-Dependent Differential Gene Expression Profiles of Cranial Neural Crest Cells Derived from Mouse Induced Pluripotent Stem Cells

Ayano Odashima[1 ¶], Shoko Onodera[2], Akiko Saito[2], Takashi Nakamura[2], Yuuki Ogihara[3], Tatsuya Ichinohe[3], Toshifumi Azuma[1,2*]

[1] Department of Oral Health Science Center, Tokyo Dental College, Tokyo, Japan

[2] Department of Biochemistry, Tokyo Dental College, Tokyo, Japan

[3] Department of Dental Anesthesiology, Tokyo Dental College, Tokyo, Japan

¶ These authors contributed equally to this work.

*Corresponding author

E-mail satouayano@tdc.ac.jp

bioRxiv preprint doi: https://doi.org/10.1101/432302; this version posted October 1, 2018. The copyright holder for this preprint (which was not certified by peer review) is the author/funder, who has granted bioRxiv a license to display the preprint in perpetuity. It is made available under aCC-BY 4.0 International license.

Abstract

Cranial neural crest cells (cNCCs) comprise a multipotent population of cells that migrate into the pharyngeal arches of the vertebrate embryo and differentiate into a broad range of derivatives of the craniofacial organs. Consequently, migrating cNCCs are considered as one of the most attractive candidate sources of cells for regenerative medicine. In this study, we analyzed the gene expression profiles of cNCCs at different time points after induction by conducting three independent RNA sequencing experiments. We successfully induced cNCC formation from mouse induced pluripotent stem (miPS) cells by culturing them in neural crest inducing media for 14 days. We found that these cNCCs expressed several neural crest specifier genes but were lacking some previously reported specifiers, such as paired box 3 (*Pax3*), msh homeobox 1 (*Msx1*), and Forkhead box D3 (*FoxD3*), which are presumed to be essential for neural crest development in the embryo. Thus, a distinct molecular network may the control gene expression in miPS-derived cNCCs. We also found that *c-Myc*, ETS proto-oncogene 1, transcription factor (*Ets1*), and sex determining region Y-box 10 (*Sox10*) were only detected at 14 days after induction. Therefore, we assume that these genes would be useful markers for migratory cNCCs induced from miPS cells. Eventually, these cNCCs comprised a broad spectrum of protocadherin (Pcdh) and a disintegrin and metalloproteinase with thrombospondin motifs (Adamts) family proteins, which may be crucial in their migration.

bioRxiv preprint doi: https://doi.org/10.1101/432302; this version posted October 1, 2018. The copyright holder for this preprint (which was not certified by peer review) is the author/funder, who has granted bioRxiv a license to display the preprint in perpetuity. It is made available under aCC-BY 4.0 International license.

Introduction

Stem cell-based tissue engineering is important in the field of oral science as it allows the regeneration of damaged tissues or organs [1,2]. Various stem cell populations have been identified as having a regeneration potential in the craniofacial region; however, the cranial neural crest cells (cNCCs) are considered as one of the most important candidates due to their role in craniofacial tissue organization [3].

cNCCs comprise a multipotent population of migratory cells that are unique to the vertebrate embryo and give rise to a broad range of derivatives [4,5], with the neural crest (NC) being capable of forming teratoma when transplanted into the immunocompromised animals [6]. The development of cNCCs involves three stages [7–10]: the neural plate border stage, the premigratory stage, and the migratory stage. During the migratory stage, the cNCCs delaminate from the posterior midbrain and individual rhombomeres in the hindbrain [11] and migrate into the pharyngeal arches to form skeletal elements of the face and teeth and contribute to the pharyngeal glands (thymus, thyroid, and parathyroid) [12]. Consequently, presumably cNCCs may represent a new treatment strategy for diseases in the craniofacial region [13].

Development from the premigratory to migratory stage proceeds swiftly [14], making it difficult to isolate and characterize a pure cNCC population from the embryo [15]. A recent transcriptome analysis of pure populations of sex determining region Y-box 10 (*Sox10*) +

bioRxiv preprint doi: https://doi.org/10.1101/432302; this version posted October 1, 2018. The copyright holder for this preprint (which was not certified by peer review) is the author/funder, who has granted bioRxiv a license to display the preprint in perpetuity. It is made available under aCC-BY 4.0 International license.

59 migratory cNCCs from chicks [16] has greatly improved our understanding of the characteristics
60 of cNCCs, and methods for deriving NCCs from the embryonic stem (ES) cells have also been
61 reported [17–30]; however, it remains unclear whether these cells are in the migratory stage and
62 how long it takes to promote ES cell-derived NCCs from the pre-migratory to migratory stage.
63 In recent years, the use of induced pluripotent stem (iPS) cells as a revolutionary approach
64 to the treatment of various medical conditions has gained immense attention [31,32] and iPS cells
65 have several clear advantages over ES cells and primary cultured cNCCs as a cell source in
66 regenerative medicine [16]. NCCs have been generated from iPS cells in numerous ways [24,33–
67 38], with two reports having examined the differentiation of NCCs from ES or iPS cells [24,39]
68 and two articles having described the protocol for differentiating NCCs from mouse iPS (miPS)
69 cells [33,34]; however, few studies have investigated the changes in the properties of these NCCs
70 overtime during the dynamic differentiation processes in the NC, in particular, during the
71 migratory stage. Embryonic NC development depends on several environmental factors that
72 influence the NC progenitors, regulation, and the timing of differentiation, making the elucidation
73 of the gene regulatory network and expression profiles of miPS cell-derived cNCCs important.
74 Recent advances in the next-generation RNA sequencing technology (RNA-seq) have made
75 it possible to analyze the gene expression profiles comprehensively [40–42]. Therefore, here, we
76 used RNA-seq to investigate the gene expression landscape of cNCCs induced from miPS cells.

bioRxiv preprint doi: https://doi.org/10.1101/432302; this version posted October 1, 2018. The copyright holder for this preprint (which was not certified by peer review) is the author/funder, who has granted bioRxiv a license to display the preprint in perpetuity. It is made available under aCC-BY 4.0 International license.

77 We treated the iPS-derived cells with cNCC induction medium for 14 days and performed
78 triplicate RNA-seq experiments. We found that standard NC markers such as nerve growth factor
79 receptor (*Ngfr*), snail family transcriptional repressor 1 (*Snai1*), and *Snai2* were remarkably
80 increased at 7 days after cNCC induction; whereas, the expression of the cNCC markers ETS
81 proto-oncogene 1, transcription factor (*Ets1*), and *Sox5*, *-8*, *-9*, and *-10* characteristically increased
82 at 14 days after cNCC induction. Nestin (*Nes*) was upregulated throughout cNCC differentiation,
83 as described previously [23]. In contrast, the homeobox genes such as msh homeobox 1 (*Msx1*),
84 paired box 3 (*Pax3*), and *Pax7* were not detected in the NC after a longer period of differentiation,
85 despite their expressions having been observed in several animals [43–52]. Furthermore, the
86 expression of Forkhead box D3 (*FoxD3*), which is known to be required for maintaining
87 pluripotency in mouse ES cells [53] and is also an important NC specifier transcription factor
88 during embryonic development, decreased over time, suggesting that it is not a cNCC specifier in
89 iPS-derived cells.

90 Another important finding was the remarkable upregulation of several metzincins, including
91 members of the disintegrin and metalloproteinase domain metallopeptidase with thrombospondin
92 motifs (Adamts) metalloproteinase family, which play crucial roles in modulating the
93 extracellular matrix (ECM) during development [54–56]. We assume that various kinds of
94 Adamts proteins produce distinct extracellular proteins that are digested by cNCC swallowing

bioRxiv preprint doi: https://doi.org/10.1101/432302; this version posted October 1, 2018. The copyright holder for this preprint (which was not certified by peer review) is the author/funder, who has granted bioRxiv a license to display the preprint in perpetuity. It is made available under aCC-BY 4.0 International license.

95 them to easily migrate toward their final destinations. We also found that the expressions of nearly
96 all procadherin (Pcdh) superfamily members were increased, some only at the migratory stage.
97 Pcdh is the largest subfamily of cadherins and the digestion of Pcdh protein by Adam proteins is
98 crucial for development [57].

99 Eventually, our results indicated that *c-Myc*; *Ets1*; *Sox10; Adamts2* and *-8*; protocadherin
100 alpha 2 (*Pcdha2*); *Pcdha5*, *-7*, *-11*, and *-12*; protocadherin alpha subfamily C,1 (*Pcdhac1*); and
101 protocadherin gamma subfamily C, 3 (*Pcdhgc3*) may represent appropriate markers for migratory
102 cNCCs induced from miPS cells.

103

104 Materials and Methods

105 miPS cell culture

106 All of the mouse studies were conducted in accordance with protocols approved by the
107 Animal Research Committee of Tokyo Dental College (No. 270401).

108 The miPS cells that were used in this study (APS0001; iPS-MEF-Ng-20D-17 mouse induced
109 pluripotent stem cell line) were purchased from RIKEN BRC (Ibaraki, Japan) [58]. The cells were
110 maintained on inactivated murine embryonic fibroblast (MEF) feeder cells in Dulbecco's
111 Modified Eagle's Medium (DMEM; Invitrogen, Carlsbad, CA, USA)supplemented with 15%
112 KnockOut™ Serum Replacement (Invitrogen), 1% nonessential amino acids (Chemicon,

bioRxiv preprint doi: https://doi.org/10.1101/432302; this version posted October 1, 2018. The copyright holder for this preprint (which was not certified by peer review) is the author/funder, who has granted bioRxiv a license to display the preprint in perpetuity. It is made available under aCC-BY 4.0 International license.

113 Temecula, CA, USA), 1% L-glutamine (Chemicon), 1000 U/ml penicillin–streptomycin (P/S;
114 Invitrogen), and 0.11 mM 2-mercaptoethanol (Wako Pure Chemical Industries Ltd., Osaka,
115 Japan) and were passaged in 60-mm cell culture plates at a density of 1×10^5 cells/plate. The cells
116 were grown in 5% CO_2 at 95% humidity and the culture medium was changed each day.
117

118 Embryoid body (EB) formation and cNCC differentiation

119 We obtained cultured cNCC cells following a previously described procedure [59], as
120 outlined in Fig 1. miPS cells were dissociated with 0.05% trypsin–ethylenediaminetetraacetic acid
121 (EDTA; Invitrogen) and were transferred to low-attachment, 10-mm petri dishes at a density of 2
122 $\times 10^6$ cells/plate to generate EBs. The EBs were then cultured in the NC induction medium
123 comprising a 1:1 mixture of DMEM and F12 nutrient mixture (Invitrogen) and Neurobasal™
124 medium (Invitrogen) supplemented with 0.5 × N2 (Invitrogen), 0.5 × B27 (Invitrogen), 20 ng/ml
125 basic fibroblast growth factor (Reprocell, Yokohama, Japan), 20 ng/ml epidermal growth factor
126 (Peprotech, Offenbach, Germany), and 1% penicillin–streptomycin (P/S) for 4 days, during which
127 time the medium was changed every other day. After 4 days, the day 0 (d0) EBs were collected
128 and plated on 60-mm cell culture plates coated with 1μg/ml collagen type I (Advanced BioMatrix,
129 San Diego, CA, USA). The cells were then subcultured in the same medium, which was changed
130 every other day, and any rosetta-forming cells were eliminated. After 7–10 days, d7 cells were

bioRxiv preprint doi: https://doi.org/10.1101/432302; this version posted October 1, 2018. The copyright holder for this preprint (which was not certified by peer review) is the author/funder, who has granted bioRxiv a license to display the preprint in perpetuity. It is made available under aCC-BY 4.0 International license.

131 dissociated with 0.05% trypsin–EDTA and transferred to 60-mm cell culture plates coated with
132 1μg/ml collagen type I at a density of 1×10^5 cells/plate to generate 14 cells. The cells from each
133 of these passages were collected for RNA extraction.
134
135 **Fig 1. The experimental protocol that was used to induce the formation of cranial neural**
136 **crest cells (cNCCs) from mouse induced pluripotent stem (miPS) cells.** The photographs
137 reveal miPS cells at four different stages: initial miPS cells, embryoid body (EB) on day 0 (d0),
138 and cNCCs on d7 and d14. Small circles represent miPS cells; large circles represent EBs; ellipses
139 represent d7 and d14 cells. Scale bar = 50 μm.
140

141 O9-1 cell culture

142 O9-1 cells, which area mouse cNCC line, were purchased from Milliopore (Billerica, MA,
143 USA) and cultured as previously described [50] as a control.
144

145 RNA isolation and quantitative reverse transcription
146 polymerase chain reaction analysis

147 The representative NC markers *Ngfr*, *Snai1*, *Snai2*, *Sox9*, and *Sox10* were selected and
148 analyzed by quantitative reverse transcription polymerase chain reaction (qRT-PCR) analysis.

bioRxiv preprint doi: https://doi.org/10.1101/432302; this version posted October 1, 2018. The copyright holder for this preprint (which was not certified by peer review) is the author/funder, who has granted bioRxiv a license to display the preprint in perpetuity. It is made available under aCC-BY 4.0 International license.

149 Total RNA was extracted using QIAzol® reagent (Qiagen, Valencia, CA, USA) according to the
150 manufacturer's protocol and RNA purity was assessed using a NanoDrop® ND-1000
151 spectrophotometer (Thermo Fisher Scientific, Waltham, MA, USA), which revealed that each
152 RNA sample had an A260/A280 ratio of >1.9. Complementary DNA (cDNA) was synthesized
153 using a high-capacity cDNA reverse transcription kit (Applied Biosystems, Foster City, CA,
154 USA) and qRT-PCR analysis was performed using Premix Ex Taq™ reagent (Takara Bio Inc.,
155 Otsu, Japan) according to the manufacturer's protocol and the Applied Biosystems® 7500 Fast
156 Real-Time PCR System, with the primer sequences presented in Table 1. All samples were
157 normalized to levels of 18S ribosomal RNA (*18S rRNA*). The relative expressions of the genes of
158 interest were analyzed using the $\Delta\Delta Ct$ method and were compared among the groups using
159 analysis of variance (ANOVA) followed by the Bonferroni test where the significant differences
160 were detected among the groups. A significance level of $p < 0.05$ was used for all analyses and
161 all data are expressed as means ± standard deviations (SD).
162
163 **Table 1. Primers used for quantitative reverse transcription polymerase chain reaction**
164 **(qRT-PCR).**

Gene	Forward primer sequence	Reverse primer sequence
18S rRNA	CGGACAGGATTGACAGATTG	CGCTCCACCAACTAAGAACG
Ngfr(p75NTR)	ACTGAGCGCCAGTTACGC	CGTAGACCTTGTGATCCATCG
Snai1 (*Snail*)	CTTGTGTCTGCACGACCTGT	AGGAGAATGGCTTCTCACCA
Snai2 (*Slug*)	CATTGCCTTGTGTCTGCAAG	CAGTGAGGGCAAGAGAAAGG

bioRxiv preprint doi: https://doi.org/10.1101/432302; this version posted October 1, 2018. The copyright holder for this preprint (which was not certified by peer review) is the author/funder, who has granted bioRxiv a license to display the preprint in perpetuity. It is made available under aCC-BY 4.0 International license.

Sox9	GTACCCGCATCTGCACAAC	CTCCTCCACGAAGGGTCTCT
Sox10	ATGTCAGATGGGAACCCAGA	GTCTTTGGGGTGGTTGGAG

Immunohistochemistry

The cells were fixed with 4% paraformaldehyde (Wako Pure Chemical Industries Ltd.) for 15 min followed by methanol (Wako Pure Chemical Industries Ltd) for 5 min. After washing, the nonspecific binding of antibodies was blocked by adding 5% bovine serum albumin (BSA; Wako Pure Chemical Industries Ltd.) in a phosphate buffered saline (PBS) with 0.5% Triton X-100 (PBST) for 1 h. The cells were then incubated with the primary antibodies Snai1 1:50 for goat anti-rabbit (Proteintech Group, Inc. Chicago, Il, USA) and Sox10 1:500 for goat anti-mouse (Atlas Antibodies, Bromma, Sweden) in PBST for 2 nights at 4 °C. They were then incubated in the secondary antibodies fluorenscein isothiocyanate conjugated anti-rabbit IgG (Abcam, Cambridge, MA, USA) at a dilution of 1:500 for Snai1 and anti-mouse IgG (Invitrogen) at a dilution of 1:500 for Sox10 in PBST for 1 h. Eventually, the cells were stained with 4,6-diamidino-2-phenylindole (DAPI; Sigma, Livonia, MI, USA) to visualize the nuclear DNA.

RNA-seq and analysis

Total RNA from each sample was used to construct libraries with the Illumina TruSeq Stranded mRNA LT Sample Prep Kit (Illumina, San Diego, CA, USA), according to the

bioRxiv preprint doi: https://doi.org/10.1101/432302; this version posted October 1, 2018. The copyright holder for this preprint (which was not certified by peer review) is the author/funder, who has granted bioRxiv a license to display the preprint in perpetuity. It is made available under aCC-BY 4.0 International license.

manufacturer's instructions. Polyadenylated mRNAs are commonly extracted using oligo-dT beads, following which the RNA is often fragmented to generate reads that cover the entire length of the transcripts. The standard Illumina approach relies on randomly primed double-stranded cDNA synthesis followed by end-repair, ligation of dsDNA adapters, and PCR amplification. The multiplexed libraries were sequenced as 125-bp paired-end reads using the Illumina Hiseq2500 system (Illumina). Prior to performing any analysis, we confirmed the quality of the data and undertook read cleaning, such as adapter removal and simple quality filtering, using Trimmomatic (ver. 0.32). The paired-end reads were then mapped to the mouse genome reference sequence GRCm38 using the Burrows–Wheeler Aligner (ver. 0.7.10). The number of sequence reads that were mapped to each gene domain using SAM tools (ver. 0.1.19) was counted and the reads per kilobase of transcript per 1 million mapped reads (RPKM) for known transcripts were calculated to normalize the expression level data to gene length and library size, allowing different samples to be compared.

Results

Gene expression profiles and immunohistochemistry of cNCCs differentiated from miPS cells

The expressions of the NC markers *Ngfr*, *Snai1*, *Snai2*, *Sox9*, and *Sox10* were examined by

bioRxiv preprint doi: https://doi.org/10.1101/432302; this version posted October 1, 2018. The copyright holder for this preprint (which was not certified by peer review) is the author/funder, who has granted bioRxiv a license to display the preprint in perpetuity. It is made available under aCC-BY 4.0 International license.

200 qRT-PCR in cNCCs differentiated from miPS cells as well as in O9-1 cells as a control. We
201 detected the expression of all genes except *Ngfr* and *Sox10* in the O9-1 cells [50]. In contrast, all
202 five genes were detected in the cNCCs, with the premigratory neural crest markers *Ngfr*, *Snai1*,
203 and *Snai2* having the highest expression levels in d7 cells and the migratory and cranial neural
204 crest markers *Sox9* and *Sox10* having the highest levels in d14 cells (Fig. 2A).
205 The strongest immunofluorescent staining was detected in d7 cells for Snai1 and d14 cells
206 for Sox10 (Fig 2B).
207
208 **Fig 2. Comparison between O9-1 cells and cranial neural crest cells (cNCCs) derived from**
209 **mouse induced pluripotent stem (miPS) cells using quantitative reverse transcription**
210 **polymerase chain reaction (qRT-PCR) and immunostaining.** (A) Expression of the
211 premigratory neural crest (NC) markers *Ngfr*, *Snai1*, and *Snai2* and the migratory NC and cNC
212 markers *Sox9* and *Sox10*. Expressions of the premigratory NC markers increased in day 7 (d7)
213 cells, whereas those of the migratory markers increased in d14 cells. *Sox10* was not detected in
214 the O9-1 cells. Each experiment was performed in triplicate with values representing the mean ±
215 SD. Groups were compared using ANOVA followed by the Bonferroni test: $*p < 0.05$. (B)
216 Immunostaining of d7 and d14 cells. Sox10 was more highly expressed in d14 cells, whereas
217 Snai1

bioRxiv preprint doi: https://doi.org/10.1101/432302; this version posted October 1, 2018. The copyright holder for this preprint (which was not certified by peer review) is the author/funder, who has granted bioRxiv a license to display the preprint in perpetuity. It is made available under aCC-BY 4.0 International license.

NC specifier transcription factors

We conducted a literature search of NC specifier transcription factors that have been identified *in vivo* [16, 43–52, 60–106] (Tables 2 and 3) and compared these with our RNA-seq results. The relative expressions of genes that underwent a significant change in expression are presented in Fig 3A.

Table 2. Cranial neural crest cells (cNCCs) genes that have previously been examined in vivo.

	Reference		Vertebrates					RNA-seq	
			L	*Z*	*X*	*C*	*M*	d7	d14
Sox10	60	Antonellis A et al., 2006				○		×	○
	61	Betancur P et al., 2010				○			
	62	Rinon A et al., 2011				○			
	63	Hari L et al., 2012					○		
	16	Simões-Costa M et al., 2014				○			
	64	Murko C et al., 2016					○		
Sox9	65	Spokony RF et al., 2002		○				○	○
	63	Hari L et al., 2012					○		
Sox8	16	Simões-Costa M et al., 2014				○		○	○
Sox5	66	Perez-Alcala S et al., 2004				○		○	○
Snai2	63	Hari L et al., 2012					○	○	×
	16	Simões-Costa M et al., 2014				○			
Ets1	61	Betancur P et al., 2010				○		×	○
	67	Meyer B et al., 2013				○			
Zic1	68	Nagai T et al., 1997					○	○	×
Zic2	68	Nagai T et al., 1997					○	×	×
	69	Teslla JJ et al., 2013		○					

bioRxiv preprint doi: https://doi.org/10.1101/432302; this version posted October 1, 2018. The copyright holder for this preprint (which was not certified by peer review) is the author/funder, who has granted bioRxiv a license to display the preprint in perpetuity. It is made available under aCC-BY 4.0 International license.

Zic3	67	Nagai T et al., 1997					○	×	×
Lmo4	16	Simões-Costa M et al., 2014				○		×	×
Rxrg	16	Simões-Costa M et al., 2014				○		×	○
Ltk	16	Simões-Costa M et al., 2014				○		×	×
Col9a3	16	Simões-Costa M et al., 2014				○		×	○
Id2	70	Das A et al., 2012		○				○	○
	16	Simões-Costa M et al., 2014				○			
Ebf1	16	Simões-Costa M et al., 2014				○		○	×
Alex1	16	Simões-Costa M et al., 2014				○		×	×
Lhx9	16	Simões-Costa M et al., 2014				○		×	×
Twist1	70	Das A et al., 2012		○				○	○
Meis2	71	Machon O et al., 2015					○	○	○

226

L	*Lamprey*
Z	*Zebrafish*
X	*Xenopus*
C	*Chick*
M	*Mouse*

227 Open circles indicate genes that were upregulated on day 7 (d7) or d14 compared with d0 [log fold
228 change (FC) > 1, $p < 0.01$, false discovery rate (FDR) < 0.05), whereas crosses indicate genes that
229 were not upregulated.

230

231 **Table 3. Neural crest (NC) transcription factors that have previously been examined *in vivo*.**

	Reference		Vertebrates					Stage			RNA-seq	
			L	*Z*	*X*	*C*	*M*	N	P	M	d7	d14
Ap2	72	Mitchell PJ et al.,1991					○	○			○	×
	73	Shen H et al., 1997				○		○				
	74	Luo T et al., 2003			○			○				
	43	Sauka-Spengler T et al., 2007	○						○			
	44	Nikitina N et al., 2008	○					○				
	45	Khudyakov J et al., 2010			○			○	○	○		

bioRxiv preprint doi: https://doi.org/10.1101/432302; this version posted October 1, 2018. The copyright holder for this preprint (which was not certified by peer review) is the author/funder, who has granted bioRxiv a license to display the preprint in perpetuity. It is made available under aCC-BY 4.0 International license.

	75	de Crozé N et al., 2011		○				○				
	76	Wang WD et al., 2011		○				○				
	77	Powell DR et al.,2013		○				○				
Dlx5	78	Yang L et al., 1998					○	○			○	○
	79	Luo T et al., 2001			○			○				
	43	Sauka-Spengler T et al., 2007	○					○				
	45	Khudyakov J et al., 2010				○		○				
Dlx3	43	Sauka-Spengler T et al., 2007	○					○			×	×
	45	Khudyakov J et al., 2010				○		○				
Gbx2	80	Li B et al., 2009			○			○			×	×
N-myc	44	Nikitina N et al., 2008	○					○			×	×
	45	Khudyakov J et al., 2010				○		○				
Msx1	46	Hill RE et al., 1989					○	○			×	×
	47	Suzuki A et al., 1997			○			○				
	43	Sauka-Spengler T et al., 2007	○					○				
	44	Nikitina N et al., 2008	○					○				
	45	Khudyakov J et al., 2010				○		○	○	○		
	48	Simões-Costa M et al., 2012				○		○				
Pax3	49	Goulding MD et al., 1991					○	○	○		○	×
	50	Bang AG et al., 1999			○			○				
	43	Sauka-Spengler T et al., 2007	○					○				
	44	Nikitina N et al., 2008	○					○	○			
	48	Simões-Costa M et al.,2012				○		○				
	51	Alkobtawi M et al., 2018			○			○	○			
Pax7	43	Sauka-Spengler T et al., 2007	○					○			○	×
	44	Nikitina N et al., 2008	○					○				
	45	Khudyakov J et al., 2010				○		○	○	○		
	52	Maczkowiak F et al., 2010			○			○	○			
	48	Simões-Costa M et al., 2012				○		○				
Zic1	68	Nagai T et al., 1997					○	○	○		○	×
	81	Nakata K et al., 1998		○				○				
	43	Sauka-Spengler T et al., 2007	○					○				
	44	Nikitina N et al., 2008	○					○				
	45	Khudyakov J et al., 2010				○		○				

bioRxiv preprint doi: https://doi.org/10.1101/432302; this version posted October 1, 2018. The copyright holder for this preprint (which was not certified by peer review) is the author/funder, who has granted bioRxiv a license to display the preprint in perpetuity. It is made available under aCC-BY 4.0 International license.

Zic2	68	Nagai T et al., 1997					○	○	○		×	×
	81	Nakata K et al., 1998		○				○				
	43	Sauka-Spengler T et al., 2007	○					○				
Zic3	68	Nagai T et al., 1997					○	○	○		×	×
	81	Nakata K et al., 1998		○				○				
	43	Sauka-Spengler T et al., 2007	○					○				
FoxD3	82	Dottori M et al., 2001					○		○	○	×	×
	83	Kos R et al., 2001				○			○			
	43	Sauka-Spengler T et al., 2007	○							○		
	45	Khudyakov J et al., 2010				○		○	○	○		
	76	Wang WD et al., 2011		○				○				
	48	Simões-Costa M et al., 2012				○				○		
	77	Powell DR et al., 2013		○				○				
Meis2	71	Machon O et al., 2015					○	○	○		○	○
Ngfr	84	Wilson YM et al., 2004					○		○		○	×
Pdgfa	85	Liu L et al., 2002		○					○		○	○
Id2	86	Liu KJ et al., 2003			○					○	○	○
	43	Sauka-Spengler T et al., 2007	○						○			
	70	Das A et al., 2012		○					○			
	16	Simões-Costa M et al., 2014				○				○		
Id3	86	Liu KJ et al., 2003			○					○	○	○
	43	Sauka-Spengler T et al., 2007	○						○			
Id4	43	Sauka-Spengler T et al., 2007	○						○		○	○
c-Myc	43	Sauka-Spengler T et al., 2007	○						○		×	○
	45	Khudyakov J et al., 2010				○		○	○	○		
Pfkfb4	87	Figueiredo AL et al., 2017			○				○		○	○
Elp3	88	Yang X et al., 2016		○					○	○	×	×
Snai1	89	Sefton M et al., 1998				○	○		○		○	×
	90	del Barrio MG et al., 2002				○			○	○		
	91	Aybar MJ et al., 2003			○					○		
	43	Sauka-Spengler T et al., 2007	○						○			
Snai2	92	Nieto MA et al., 1994				○			○		○	×
	93	Jiang R et al., 1998					○			○		
	90	del Barrio MG et al., 2002				○			○	○		

bioRxiv preprint doi: https://doi.org/10.1101/432302; this version posted October 1, 2018. The copyright holder for this preprint (which was not certified by peer review) is the author/funder, who has granted bioRxiv a license to display the preprint in perpetuity. It is made available under aCC-BY 4.0 International license.

	91	Aybar MJ et al., 2003			○					○		
	45	Khudyakov J et al., 2010				○			○	○		
	94	Tien CL et al., 2015			○					○		
Ets1	43	Sauka-Spengler T et al., 2007	○							○	×	○
Sox5	95	Martin BL et al., 2001			○					○	○	○
	67	Perez-Alcala S et al., 2004				○			○	○		
Sox6	67	Perez-Alcala S et al., 2004				○			○	○	○	○
Sox8	43	Sauka-Spengler T et al., 2007	○							○		
Sox9	96	Cheung M et al., 2003				○				○	○	○
	97	Cheung M et al., 2005				○			○	○		
	43	Sauka-Spengler T et al., 2007	○							○		
	61	Betancur P et al., 2010				○				○		
Sox10	98	Honoré SM et al., 2003			○					○	×	○
	99	McKeown SJ et al., 2005					○			○		
	43	Sauka-Spengler T et al., 2007	○							○		
	61	Betancur P et al., 2010				○				○		
	100	Prasad MK et al., 2011		○						○		
	63	Hari L et al., 2012					○			○		
	16	Simões-Costa M et al., 2014				○				○		
	101	Baggiolini A et al., 2015				○				○		
	94	Tien CL et al., 2015			○					○		
	51	Alkobtawi M et al., 2018			○					○		
Lmo4	16	Simões-Costa M et al., 2014				○				○	×	×
Rxrg	16	Simões-Costa M et al., 2014				○				○	×	○
Ltk	16	Simões-Costa M et al., 2014				○				○	×	×
Col9a3	16	Simões-Costa M et al., 2014				○				○	×	○
Alex1	16	Simões-Costa M et al., 2014				○				○	×	×
Ebf1	16	Simões-Costa M et al., 2014				○				○	○	×
Lhx9	16	Simões-Costa M et al., 2014				○				○	×	×
Erbb3	100	Prasad MK et al., 2011		○						○	×	×
Ang2	102	McKinney MC et al., 2016				○				○	×	×
Ednrb	103	Lee HO et al., 2003					○			○	×	○
Hnk1	104	Giovannone D et al., 2015				○				○	○	○
Twist1	43	Sauka-Spengler T et al., 2007	○							○	○	○

bioRxiv preprint doi: https://doi.org/10.1101/432302; this version posted October 1, 2018. The copyright holder for this preprint (which was not certified by peer review) is the author/funder, who has granted bioRxiv a license to display the preprint in perpetuity. It is made available under aCC-BY 4.0 International license.

Slit1	105	Zuhdi N et al., 2012				○				○	○	○
Slit2	105	Zuhdi N et al., 2012				○				○	○	○
Slit3	105	Zuhdi N et al., 2012				○				○	○	×

232

Vertebrates		Stages	
L	*Lamprey*	N	Neural plate border
Z	*Zebrafish*	P	Premigratory neural crest
X	*Xenopus*	M	Migratory neural crest
C	*Chick*		
M	*Mouse*		

233

234 Open circles indicate genes that were upregulated on day 7 (d7) or d14 compared with d0 [log fold
235 change (FC) >1, $p < 0.01$, false discovery rate (FDR) < 0.05), whereas crosses indicate genes that were
236 not upregulated.

237

238 **Fig 3. RNA sequencing results for cranial neural crest cells (cNCCs) differentiated from**
239 **mouse induced pluripotent stem (miPS) cells.** (A) Expression of each of the genes listed in
240 Table 2 at day 0 (d0), d7, and d14 after induction. Sex-determining region Y (SRY)-related high
241 mobility group (HMG) box genes were most upregulated in d14 cells. The vertical axis reveals
242 reads per kilobase of exon per million mapped reads (RPKM) and the horizontal axis indicates
243 time. Each experiment was performed in triplicate with values representing the mean ± SD.
244 Groups were compared using ANOVA followed by the Bonferroni test: *$p < 0.05$. (B) Expression
245 of genes that have not been examined during the neural crest stages *in vivo*. *Tnc* was most

bioRxiv preprint doi: https://doi.org/10.1101/432302; this version posted October 1, 2018. The copyright holder for this preprint (which was not certified by peer review) is the author/funder, who has granted bioRxiv a license to display the preprint in perpetuity. It is made available under aCC-BY 4.0 International license.

upregulated in the d14 cells, whereas *Cha6* and *Rhob* were upregulated in the d7 cells. The vertical axis reveals reads per kilobase of exon per million mapped reads (RPKM) and the horizontal axis indicates time. Open circles indicate genes that were upregulated on day 7 (d7) or d14 compared with d0 [log fold change (FC) > 1, $p < 0.01$, false discovery rate (FDR) < 0.05). Each experiment was performed in triplicate with values representing the mean ± SD. Groups were compared using ANOVA followed by the Bonferroni test: $*p < 0.05$.

We found that the *transcription factor AP-2 alpha* (*Ap2*) along with *Pax3* and zinc finger protein of the cerebellum 1 (*Zic1*), both of which are regulated by *Ap2*, were most highly expressed in d7 cells (Fig 3A). *Pax6*, which has been reported in human ES and iPS-derived NC cells (Tables 2 and 3), was detected in both d7 and d14 cells, whereas *Pax7*, which has not previously been reported in the mouse NC, was also detected in the d7 cells (Fig 3A). In contrast, the homeobox genes *gastrulation brain homeobox 2 (Gbx2), Msx1, distal-less homeobox 3 (Dlx3), Zic2*, and *Zic3* were not detected in d7 or d14 cells, and the homeobox genes *Zic1* and *Dlx5* were only expressed in d7 cells, despite these having been reported in the NC of a range of species (Table 2); however, *Meis homeobox 2 (Meis2)* was expressed in both d7 and d14 cells.

Both MYCN proto-oncogene, bHLH transcription factor (*N-myc*) and *c-Myc* have been reported in NCCs (Table 3); however, we did not observe *N-myc* expression in d7 or d14 cells

bioRxiv preprint doi: https://doi.org/10.1101/432302; this version posted October 1, 2018. The copyright holder for this preprint (which was not certified by peer review) is the author/funder, who has granted bioRxiv a license to display the preprint in perpetuity. It is made available under aCC-BY 4.0 International license.

and detected *c-Myc* expression in the d7 and d14 group (Fig 3A). Furthermore, we observed substantial downregulation of the winged-helix transcription factor *FoxD3* over time (Fig 3A), which is an important factor for maintaining the pluripotency of ES cells and a key NC specifier that has been implicated in multiple steps of NC development and NCC migration in the embryo of various species (Table 2).

The premigratory NC markers *Ngfr*, heart and neural crest derivatives expressed 2 (*Hand2*), *Snai1*, and *Snai2* were only detected in the d7 cells; however, other premigratory NC markers, such as platelet derived growth factor receptor, alpha polypeptide (*Pdgfra*), 6-phosphofructo-2-kinase/fructose-2,6-biphosphatase 4 (*Pfkfb4*), inhibitor of DNA binding 2 (*Id2*), *Id3*, and *Id4* were found in both d7 and d14 cells, as was *Nes* (Fig 3A).

Migratory neural crest markers expression of *Sox5*, *-6*, *-8*, *-9*, and *-10*, which encode members of the sex-determining region Y (SRY)-related high mobility group (HMG)-box family of transcription factors and have been reported to be crucial in several aspects of NCCs, were observed in d7 or d14 cells. *Sox10*, which is a known marker of migratory cNCCs in various species (Table 2), was only detected in d14 cells, as were other migratory NC markers, including retinoid X receptor gamma (*Rxrg*), collagen type IX alpha 3 chain (*Col9a3*), and endothelin receptor type B (*Ednrb*; Fig. 3A); however, LIM domain only 4 (*Lmo4*), leukocyte tyrosine kinase (*Ltk*), erb-b2 receptor tyrosine kinase 3 (*Erbb3*), and angiogenin, ribonuclease A family, member

bioRxiv preprint doi: https://doi.org/10.1101/432302; this version posted October 1, 2018. The copyright holder for this preprint (which was not certified by peer review) is the author/funder, who has granted bioRxiv a license to display the preprint in perpetuity. It is made available under aCC-BY 4.0 International license.

2 (*Ang2*) were not detected in the d14 cells.

Twist family bHLH transcription factor 1 (*Twist1*), which is activated by a variety of signal transduction pathways and is crucial in the downregulation of E-cadherin expression, was detected in both d7 and d14 cells, as was beta-1,3-glucuronyltransferase 1 (*B3gat1*/*Hnk1*), or CD57. In contrast, expression of the trunk NC markers lit guidance ligand 1/2 (*Slit1/2*), which has been reported to play an important role in the migration of trunk NC cells toward ventral sites, was upregulated only in the d7 cells (Fig 3A).

Eventually, the expressions of tenascin C (*Tnc*), cadherin-6 (*Cdh6*), and ras homolog family member B (*Rhob*), all of which are related to cell adhesion and motility [106–111], significantly increased in both d7 and d14 cells (Fig 3B).

Metzincin superfamily zinc proteinase and protocadherin superfamily expressions

Members of the metzincin superfamily are proteinases that have a zinc ion at their active site. This family includes the matrix metalloproteinases (Mmps), a disintegrin and metalloproteinase (Adam), and Adamts, all of which have attracted attention as factors involved in cancer cell invasion and cell migration. *Mmp2*, *-11*, *-14*, *-15*, *-16*, *-24*, and *-28* were significantly upregulated in the cNNCs (Fig 4A), all of which except *Mmp24* are membrane-

bioRxiv preprint doi: https://doi.org/10.1101/432302; this version posted October 1, 2018. The copyright holder for this preprint (which was not certified by peer review) is the author/funder, who has granted bioRxiv a license to display the preprint in perpetuity. It is made available under aCC-BY 4.0 International license.

bound types. The expressions of *Mmp11* and -*28* were only detected in d7 cells, while all other Mmps were detected in both d7 and d14 cells (Fig 4A, B).

Only *Adam1a*, -*8*, -*10*, and -*12* were upregulated in both d7 and d14 cells (Fig 4C, D), despite the members of this family being important in NC migration and the expressions of *Adam10*, -*12*, -*15*, -*19*, and-*33* having been observed in the mouse NC [112]. In contrast, various *Adamts* family genes, which are important for connective tissue organization and cell migration, were upregulated in either d7 or d14 cells (Fig 4C, D). The expression of *Adamts1* in particular exhibited a substantial increase in expression, while *Adamts2* and -*8*, which are presumed to be important in cancer cell invasion [55], increased in the later stages of differentiation.

Fig. 4. RNA sequencing results for the matrix metalloproteinase (*Mmp*), a disintegrin and metalloproteinase (*Adam*), and a disintegrin and metalloproteinase with thrombospondin motifs (*Adamts*) gene families. (A) Expressions of *Mmp* family genes in mouse. Round marks alongside d7 or d14 indicate that the genes were upregulated compared with d0 [log fold change (logFC) > 1, $p < 0.01$, false discovery rate (FDR) <0.05], whereas cross marks indicate no upregulation in d7 or d14 cells. (B) Graphical representation of the upregulation of *Mmp2*, -*11*, -*14*, -*15*, -*16*, -*24*, and -*28* in d7 or d14 cells. *Mmp15* and -*16* were most upregulated in d14 cells.

bioRxiv preprint doi: https://doi.org/10.1101/432302; this version posted October 1, 2018. The copyright holder for this preprint (which was not certified by peer review) is the author/funder, who has granted bioRxiv a license to display the preprint in perpetuity. It is made available under aCC-BY 4.0 International license.

318 The vertical axis reveals reads per kilobase of exon per million mapped reads (RPKM) and the
319 horizontal axis indicates time. Each experiment was performed in triplicate with values
320 representing the mean ± SD. Groups were compared using ANOVA followed by the Bonferroni
321 test: **p* < 0.05. (C) Expressions of *Adam* and *Adamts* genes in mouse. Round marks alongside d7
322 or d14 indicate that the genes were upregulated compared with d0 (logFC > 1, p < 0.01, FDR <
323 0.05), whereas cross marks indicate no upregulation. (D) Graphical representation of the
324 upregulation of *Adam1a* and *8–12*, and *Adamts1–10*, *-12*, and *15–20* in d7 or d14 cells. *Adam2*,
325 *-4*, *-7*, and *-8*, and *Adamts 9* and *-12* were most upregulated in d14 cells. The vertical axis reveals
326 reads per kilobase of exon per million mapped reads (RPKM) and the horizontal axis indicates
327 time. Each experiment was performed in triplicate with values representing the mean ± SD.
328 Groups were compared using ANOVA followed by the Bonferroni test: **p* < 0.05.
329
330 Most of the *Pcdh* genes, which are involved in cell adhesion, were upregulated in d7 and
331 d14 cells (Table 4); however, *Pcdha2*, *-5*, *-7*, *-11*, and *-12*; *Pcdhac1*; and *Pcdhgc5* were only
332 upregulated in the d14 cells.
333
334 **Table 4 Expression of the protocadherin superfamily based on RNA sequencing data.**

Pcdh	*1*	*7*	*8*	*9*	*10*	*11*	*12*	*15*	*17*	*18*	*19*	*20*
d7	×	○	○	○	○	○	×	×	○	○	○	×
d14	×	○	○	○	○	○	×	○	○	○	○	×

bioRxiv preprint doi: https://doi.org/10.1101/432302; this version posted October 1, 2018. The copyright holder for this preprint (which was not certified by peer review) is the author/funder, who has granted bioRxiv a license to display the preprint in perpetuity. It is made available under aCC-BY 4.0 International license.

Pcdha	*1*	*2*	*3*	*4*	*5*	*6*	*7*	*8*	*9*	*10*	*11*	*12*
d7	○	×	○	○	×	○	×	○	○	○	×	×
d14	○	○	○	○	○	○	○	○	○	○	○	○

Pcdhb	*1*	*2*	*3*	*4*	*5*	*6*	*7*	*8*	*9*	*10*	*11*	*12*	*13*	*14*	*15*	*16*	*17*	*18*	*19*	*20*	*21*	*22*
d7	×	○	○	○	○	○	○	○	○	○	○	○	○	○	○	○	○	○	○	○	○	○
d14	×	○	○	○	○	○	○	○	○	○	○	○	○	○	○	○	○	○	○	○	○	○

Pcdhac	*1*	*2*
d7	×	○
d14	○	○

Pcdhgc	*3*	*4*	*5*
d7	○	○	×
d14	○	○	○

Pcdhgb	*1*	*2*	*4*	*5*	*6*	*7*	*8*
d7	○	○	○	○	○	○	○
d14	○	○	○	○	○	○	○

Open circles indicate genes that were upregulated on day 7 (d7) or d14 compared with d0 [log fold change (FC) >1, $p < 0.01$, false discovery rate (FDR) < 0.05), whereas crosses indicate genes that were not upregulated.

Discussion

In this study, we successfully generated miPS-induced cNCCs that were sufficiently close to the migratory stage. The NC has previously been generated from ES or iPS cells in various ways [24,33–39] and the protocol we used in the present study was based on the methods outlined by R. Bajpai et al. [39]; however, few studies have investigated the changes in the properties of cNCCs at different time points (Table 5).

bioRxiv preprint doi: https://doi.org/10.1101/432302; this version posted October 1, 2018. The copyright holder for this preprint (which was not certified by peer review) is the author/funder, who has granted bioRxiv a license to display the preprint in perpetuity. It is made available under aCC-BY 4.0 International license.

346 **Table 5 Neural crest (NC) transcription factors that have previously been examined *in vitro*.**

347

Reference number		Mouse		Human		*Sox10*	*Snai2*	*Sox9*	*Snai1*	*Twist*	*Hnk1*	*Id2/Id3*	*Msx1*	*Ap2*	*Pax7*	*c-Myc*	*FoxD3*	*Pax3*	*Zic1*	*Ngfr*	*Pdgfra*	*Hand2*	*Msx2*	*Nes*	*Pax6*	*Ptx3*
		iPS	ES	iPS	ES																					
d7	This	○				×	○	○	○	○	○	○	×	○	○	×	×	○	○	○	○	○	×	○	○	○
d14	study					○	×	○	×	○	○	○	×	×	×	○	×	×	×	×	○	×	×	○	○	○
33		○				○								○				○		○		○				
34		○					○				○							○		○						
17			○					○					○									○				
18			○			○	○											○								
19			○			○	○	○				○				○					○					
20			○			○	○	○		○				○				○								
21			○				○	○						○						○						
24				○							○			○						○						
35				○			○				○			○						○				○		
36				○		○					○									○						
37				○			○	○			○									○					○	
38				○		○		○						○				○		○						
22					○	○							○	○			○					○				
23					○						○			○						○						
24					○						○									○						
25					○	○		○			○		○	○						○						
26					○	○	○			○				○				○				○	○			
27					○		○	○	○				○	○	○		○	○					○		○	○
28					○	○		○						○			○	○	○	○						
29					○	○					○					○				○						
30					○	○	○	○						○												

348 Open circles indicate genes that were upregulated on day 7 (d7) or d14 compared with d0 [log fold

349 change (FC) >1, $p < 0.01$, false discovery rate (FDR) < 0.05), whereas crosses indicate genes that were

350 not upregulated.

351

bioRxiv preprint doi: https://doi.org/10.1101/432302; this version posted October 1, 2018. The copyright holder for this preprint (which was not certified by peer review) is the author/funder, who has granted bioRxiv a license to display the preprint in perpetuity. It is made available under aCC-BY 4.0 International license.

352 Our d7 and d14 cells expressed typical NC markers, such as *Ngfr*, *Snai1*, and *Snai2*. In
353 contrast, the mouse cNCC line (O9-1 cells) did not express *Ngfr*, indicating that cNCCs derived
354 from miPS cells may be of better quality for evaluating the cNCC characteristics than O9-1 cells
355 [59]. We also found that, unlike O9-1 cells, d14 cells expressed considerably high levels of *Sox10*,
356 which is considered as a reliable marker for migratory cNCCs. Because cNCCs are involved in
357 organizing numerous craniofacial tissues, several reports are available on their gene expression
358 profiles; however, we found that various results that have been reported were inconsistent
359 between the species and protocols. Since cNCCs differentiate fast in the embryo [14], it is
360 considerably difficult to synchronize the timing of isolation to a particular point in their
361 development. Furthermore, migratory cNCCs intermingle with other types of cells in the embryo,
362 making it difficult to isolate and characterize a pure cell population. Consequently, there have
363 been few reports of cNCC markers [16,60–71]; however, Simoes-Costa et al. [16] successfully
364 isolated *Sox10* positive cNCCs in a chicken embryo and analyzed their gene profiles and we found
365 that d14 cells expressed several of these *Sox10* positive chicken cNCCs. It has previously been
366 suggested that NC cells have multiple populations [11] and that the generation of cNCCs from
367 iPS cells could result in numerous different populations occurring in the same dish. Therefore,
368 this diversity in populations may explain the discrepancies; however, we can conclude that under
369 the conditions used in the present study, *cMyc*; *Ets1*; *Sox10*; *Adamts2*; *Adamts8*; *Pcdha2*, *-5*, *-7*, -

bioRxiv preprint doi: https://doi.org/10.1101/432302; this version posted October 1, 2018. The copyright holder for this preprint (which was not certified by peer review) is the author/funder, who has granted bioRxiv a license to display the preprint in perpetuity. It is made available under aCC-BY 4.0 International license.

370 *11*, and-*12*; *Pcdhac1*, and *Pcdhgc3* may represent useful markers for migratory cNCCs.

371 Our results also indicated that d7 cells were still in the premigratory stage even though they
372 expressed numerous NC markers. Thus, cNCCs derived from miPS cells took more than 14 days
373 to become migratory *in vitro*, which is much slower than has been observed in the mouse embryos
374 *in vivo* under the same conditions [113].

375 RNA-seq makes it possible to normalize the expression levels of different genes, allowing
376 comparisons between samples. We conducted triplicate experiments in which none of the induced
377 cNCCs expressed several homeobox genes that are considered to be expressed in the early stages
378 of cNCC differentiation. In particular, we did not observe *FoxD3* expression in either d7 or d14
379 cells, despite it being recognized as one of the key transcription factors in cNCCs [53]. These
380 negative results indicate that cNCCs derived from miPS cells may have distinct gene regulatory
381 networks. Although it is possible that the cells would express those genes at different time points,
382 the expression of *FoxD3*, which is a pluripotent stem cell marker gene and plays an important
383 role in maintaining pluripotency, decreases in a time-dependent manner [44], making it more
384 likely that *FoxD3* may not be a key regulator in iPS-derived cNCCs. We speculate, however, that
385 iPS cells had a sufficient amount of *FoxD3* to allow them to be converted from iPS cells into
386 cNCCs.

387 Protocadherins belong to the cadherin superfamily and are involved in intercellular

bioRxiv preprint doi: https://doi.org/10.1101/432302; this version posted October 1, 2018. The copyright holder for this preprint (which was not certified by peer review) is the author/funder, who has granted bioRxiv a license to display the preprint in perpetuity. It is made available under aCC-BY 4.0 International license.

388 interactions [57], while metzincins are thought to be key proteinases that facilitate the cell
389 migration [45]. Unfortunately, the abundances of members of these families hindered their
390 analysis; however, since RNA-seq techniques enable us to evaluate the gene profiles exhaustively,
391 we were able to focus on the expressions of all of the procadherin and metazicin family members.
392 As expected, we found that several *Adam* and *Adamts* genes were upregulated, with most of the
393 latter increasing significantly. The *Adam* genes that increased in the cNCCs were the membrane-
394 bound type; whereas, the *Adamts* genes were secreted proteinases, indicating that the expression
395 of various *Adamts* may allow the matrix to be digested more efficiently, as each may be capable
396 of digesting a different type of extracellular matrix protein [45].Thus, the secretion of a variety of
397 Adamts and Pcdh proteins may play a crucial role in the migration ability of cNCCs.
398 In summary, we successfully induced the formation of cNCCs from miPS cells by placing
399 them in NC inducing media for 14 days. We found that although the resulting cNCCs had several
400 NC specifiers, some were lacking, indicating that a distinct molecular network may control the
401 gene expression in miPS-derived cNCCs. Our results also indicated that *cMyc*; *Ets1*; *Sox10*;
402 *Adamts2* and *-8*; *Pcdha2*, *-5*, *-7*, *-11*, and *-12*; *Pcdhac1*; and*Pcdhgc3* may represent appropriate
403 markers for migratory cNCCs induced from miPS cells. Eventually, these cNCCs produced a
404 broad spectrum of Adamts family proteins that may play an important role in their migration.
405

bioRxiv preprint doi: https://doi.org/10.1101/432302; this version posted October 1, 2018. The copyright holder for this preprint (which was not certified by peer review) is the author/funder, who has granted bioRxiv a license to display the preprint in perpetuity. It is made available under aCC-BY 4.0 International license.

406 # Acknowledgments

407 The author is grateful to Professor T. Azuma, MD, PhD, Department of Biochemistry, and

408 Professor T. Ichinohe, DDS, PhD, Department of Dental Anesthesiology, for their guidance. I

409 also thank S. Onodera and A. Saito, Department of Biochemistry.

410

411 # Conflict of interest

412 The authors have no conflicts of interest directly relevant to the content of this article.

413

bioRxiv preprint doi: https://doi.org/10.1101/432302; this version posted October 1, 2018. The copyright holder for this preprint (which was not certified by peer review) is the author/funder, who has granted bioRxiv a license to display the preprint in perpetuity. It is made available under aCC-BY 4.0 International license.

References

1. Luan X, Dangaria S, Ito Y, Walker CG, Jin T, Schmidt MK et al. Neural crest lineage segregation: a blueprint for periodontal regeneration. J Dent Res. 2009; 88: 781–791. https://doi.org/10.1177/0022034509340641 PMID: 19767574

2. Malhotra N. Induced Pluripotent Stem (iPS) Cells in Dentistry: A Review, Int J Stem Cells. 2016; 9: 176–185. https://doi.org/10.15283/ijsc16029 PMID: 27572712

3. Knight RD, Schilling TF. Cranial neural crest and development of the head skeleton. Adv Exp Med Biol. 2006; 589: 120–133. https://doi.org/10.1007/978-0-387-46954-67 PMID: 17076278

4. Theveneau E, Mayor R. Collective cell migration of the cephalic neural crest: the art of integrating information. Genesis. 2011; 49: 164-176. https://doi.org/10.1002/dvg.20700 PMID: 21157935

5. Chai Y, Jiang X, Ito Y, Bringas P Jr, Han J, Rowitch DH et al. Fate of the mammalian cranial neural crest during tooth and mandibular morphogenesis. Development.2000; 127: 1671–1679. PMID: 10725243

6. McConnell AM, Mito IK, Ablain J, Dang M, Formichella L, Fisher DE et al. Neural crest state activation in NRAS driven melanoma, but not in NRAS-driven melanocyte

bioRxiv preprint doi: https://doi.org/10.1101/432302; this version posted October 1, 2018. The copyright holder for this preprint (which was not certified by peer review) is the author/funder, who has granted bioRxiv a license to display the preprint in perpetuity. It is made available under aCC-BY 4.0 International license.

expansion. Dev Biol. 2018. https://doi.org/10.1016/j.ydbio.2018.05.026 PMID: 29883661

7. Meulemans D, Bronner-Fraser M. Gene- regulatory interactions in neural crest evolution and Development. Dev Cell. 2004; 7: 291–299. https://doi.org/10.1016/j.devcel.2004.08.007 PMID: 15363405

8. Steventon B, Carmona-Fontaine C, Mayor R. Genetic network during neural crest induction: from cell specification to cell survival. Semin Cell Dev Biol. 2005; 16: 647–654. https://doi.org/10.1016/j.semcdb.2005.06.001 PMID: 16084743

9. Simões-Costa M, Bronner ME. Establishing neural crest identity: a gene regulatory recipe. Development. 2015; 142: 242–257. https://dx.doi.org/10.1242%2Fdev.105445 PMID: 25564621

10. Martik ML, Bronner ME. Regulatory Logic Underlying Diversification of the Neural Crest. Trends Genet. 2017; 33: 715–727. https://doi.org/10.1016/j.tig.2017.07.015 PMID: 28851604

11. Minoux M, Rijli FM. Molecular mechanisms of cranial neural crest cell migration and patterning in craniofacial development. Development. 2010; 137: 2605–2621. https://doi.org/10.1242/dev.040048 PMID: 20663816

12. Mayor R, Theveneau E. The neural crest. Development. 2013; 140: 2247–2251. https://doi.org/10.1242/dev.091751 PMID: 23674598

bioRxiv preprint doi: https://doi.org/10.1101/432302; this version posted October 1, 2018. The copyright holder for this preprint (which was not certified by peer review) is the author/funder, who has granted bioRxiv a license to display the preprint in perpetuity. It is made available under aCC-BY 4.0 International license.

13. Okuno H, Mihara FR, Ohta S, Fukuda K, Kurosawa K, Akamatsu W et al. CHARGE syndrome modeling using patient-iPSCs reveals defective migration of neural crest cells harboring CHD7 mutations. eLife. 2017; 6: e21114 https://dx.doi.org/10.7554%2FeLife.21114 PMID: 29179815

14. Simoes-Costa M, Bronner ME. Reprogramming of avian neural crest axial identity and cell fate. Science. 2016; 352: 1570-1573. https://dx.doi.org/10.1126%2Fscience.aaf2729 PMID: 27339986

15. Milet C, Monsoro-Burq AH. Neural crest induction at the neural plate border in vertebrates. Dev Biol. 2012; 366: 22–33. https://doi.org/10.1016/j.ydbio.2012.01.013 PMID: 22305800

16. Simões-Costa M, Tan-Cabugao J, Antoshechkin I, Sauka-Spengler T, Bronner ME. Transcriptome analysis reveals novel players in the cranial neural crest gene regulatory Network. Genome Res. 2014; 24: 281–290. https://doi.org/10.1101/gr.161182.113 PMID: 24389048

17. Mizuseki K, Sakamoto T, Watanabe K, Muguruma K, Ikeya M, Nishiyama A et al. Generation of neural crest-derived peripheral neurons and floor plate cells from mouse and primate embryonic stem cells. Proc Natl Acad Sci U S A. 2003; 100: 5828–5833. https://dx.doi.org/10.1073%2Fpnas.1037282100 PMID: 12724518

18. Motohashi T, Aoki H, Chiba K, Yoshimura N, Kunisada T. Multipotent Cell Fate of Neural

bioRxiv preprint doi: https://doi.org/10.1101/432302; this version posted October 1, 2018. The copyright holder for this preprint (which was not certified by peer review) is the author/funder, who has granted bioRxiv a license to display the preprint in perpetuity. It is made available under aCC-BY 4.0 International license.

468 Crest-Like Cells Derived from Embryonic Stem Cells. Stem Cells. 2007; 25: 402–412.
469 https://doi.org/10.1634/stemcells.2006-0323 PMID: 17038669

470 19. Kawaguchi J, Nichols J, Gierl MS, Faial T, Smith A. Isolation and propagation of enteric
471 neural crest progenitor cells from mouse embryonic stem cells and embryos. Development.
472 2010; 137: 693–704. https://dx.doi.org/10.1242%2Fdev.046896 PMID: 20147374

473 20. Aihara Y, Hayashi Y, Hirata M, Ariki N, Shibata S, Nagoshi N et al. Furue, Induction of
474 neural crest cells from mouse embryonic stem cells in a serum-free monolayer culture. Int J
475 Dev Biol. 2010; l54: 1287–1294. https://doi.org/10.1387/ijdb.103173ya PMID: 20711997

476 21. Minamino Y, Ohnishi Y, Kakudo K, Nozaki M. Isolation and propagation of neural crest
477 stem cells from mouse embryonic stem cells via cranial neurospheres. Stem Cells Dev.
478 2015; 24: 172–181. https://doi.org/10.1089/scd.2014.0152 PMID: 25141025

479 22. Pomp O, Brokhman I, Ben-Dor I, Reubinoff B, Goldstein RS. Generation of peripheral
480 sensory and sympathetic neurons and neural crest cells from human embryonic stem cells.
481 Stem cells. 2005; 23: 923–930. https://doi.org/10.1634/stemcells.2005-0038 PMID:
482 15883233

483 23. Lee G, Kim H, Elkabetz Y, Al Shamy G, Panagiotakos G, Barberi T et al. Isolation and
484 directed differentiation of neural crest stem cells derived from human embryonic
485 stem cells. Nat Biotechnol. 2007; 25: 1468–1475. https://doi.org/10.1038/nbt1365 PMID:

bioRxiv preprint doi: https://doi.org/10.1101/432302; this version posted October 1, 2018. The copyright holder for this preprint (which was not certified by peer review) is the author/funder, who has granted bioRxiv a license to display the preprint in perpetuity. It is made available under aCC-BY 4.0 International license.

18037878

24. Lee G, Chambers SM, Tomishima MJ, Studer. Derivation of neural crest cells from human pluripotent stem cells. Nat Protoc. 5 (2010) 688–701. https://doi.org/10.1038/nprot.2010.35 PMID: 20360764

25. Liu Q, Spusta SC, Mi R, Lassiter RN, Stark MR, Höke A et al. Human neural crest stem cells derived from human ESCs and induced pluripotent stem cells: induction, maintenance, and differentiation into functional schwann cells. Stem Cells Transl Med. 2010; 1: 266–278. https://doi.org/10.5966/sctm.2011-0042 PMID: 23197806

26. Noisa P, Lund C, Kanduri K, Lund R, Lähdesmäki H, Lahesmaa R et al. Notch signaling regulates the differentiation of neural crest from human pluripotent stem cells. J Cell Sci. 2014; 127: 2083–2094. https://doi.org/10.1242/jcs.145755 PMID: 24569875

27. Karbalaie K, Tanhaei S, Rabiei F, Kiani-Esfahani A, Masoudi NS, Nasr-Esfahani MH et al. Stem cells from human exfoliated deciduous tooth exhibit stromal-derived inducing activity and lead to generation of neural crest cells from human embryonic stem cells. Cell J. 2015; 17: 37–48. https://dx.doi.org/10.22074%2Fcellj.2015.510 PMID: 25870833

28. Avery J, Dalton S. Methods for Derivation of Multipotent Neural Crest Cells Derived from Human Pluripotent Stem Cells. Methods Mol Biol. 2016; 1341: 197–208. https://dx.doi.org/10.1007%2F7651_2015_234 PMID: 25986498

bioRxiv preprint doi: https://doi.org/10.1101/432302; this version posted October 1, 2018. The copyright holder for this preprint (which was not certified by peer review) is the author/funder, who has granted bioRxiv a license to display the preprint in perpetuity. It is made available under aCC-BY 4.0 International license.

504 29. Zhang JT, Weng ZH, Tsang KS, Tsang LL, Chan HC, Jiang XH. MycN Is Critical for the
505 Maintenance of Human Embryonic Stem Cell-Derived Neural Crest Stem Cells. PLoS
506 One; 2016: e0148062. https://doi.org/10.1371/journal.pone.0148062 PMID: 26815535
507 30. Lovatt M, Yam GH, Peh GS, Colman A, Dunn NR, Mehta JS. Directed differentiation of
508 periocular mesenchyme from human embryonic stem cells. Differentiation. 2018; 99: 62–
509 69. https://doi.org/10.1016/j.diff.2017.11.003 PMID: 29239730
510 31. Doi D, Samata B, Katsukawa M, Kikuchi T, Morizane A, Ono Y et al. Isolation of human
511 induced pluripotent stem cell derived dopaminergic progenitors by cell sorting for successful
512 transplantation. Stem Cell Reports. 2014; 3: 337–350.
513 https://dx.doi.org/10.1016%2Fj.stemcr.2014.01.013 PMID: 24672756
514 32. Nakane T, Masumoto H, Tinney JP, Yuan F, Kowalski WJ, Ye F et al. Impact of Cell
515 Composition and Geometry on Human Induced Pluripotent Stem Cells-Derived
516 Engineered Cardiac Tissue. Sci Rep. 2017; 7: 45641.
517 https://dx.doi.org/10.1038%2Fsrep45641 PMID: 28368043
518 33. Okawa T, Kamiya H, Himeno T, Kato J, Seino Y, Fujiya A. Transplantation of Neural Crest
519 Like Cells Derived From Induced Pluripotent Stem Cells Improves Diabetic Polyneuropathy
520 in Mice. Cell Transplant. 2013; 22: 1767–1783. https://doi.org/10.3727/096368912X657710
521 PMID: 23051637

bioRxiv preprint doi: https://doi.org/10.1101/432302; this version posted October 1, 2018. The copyright holder for this preprint (which was not certified by peer review) is the author/funder, who has granted bioRxiv a license to display the preprint in perpetuity. It is made available under aCC-BY 4.0 International license.

522 34. Seki D, Takeshita N, Oyanagi T, Sasaki S, Takano I, Hasegawa M et al. Differentiation of
523 Odontoblast-Like Cells From Mouse Induced Pluripotent Stem Cells by Pax9 and Bmp4
524 Transfection Stem Cells. Transl Med. 2015: 4: 993–997.
525 https://dx.doi.org/10.5966%2Fsctm.2014-0292 PMID: 26136503
526 35. Wang A, Tang X, Li X, Jiang Y, Tsou DA, Li S. Derivation of smooth muscle cells with
527 neural crest origin from human induced pluripotent stem cells. Cells Tissues Organs.
528 2012; 195: 5–14. https://doi.org/10.1002/jcp.25437 PMID: 22005509
529 36. Kreitzer FR, Salomonis N, Sheehan A, Huang M, Park JS, Spindler MJ et al. A robust
530 method to derive functional neural crest cells from human pluripotent stem cells. Am J Stem
531 Cells. 2013; 2: 119–131. PMID: 23862100
532 37. Tomokiyo A, Hynes K, Ng J, Menicanin D, Camp E, Arthur A et al. Generation of Neural
533 Crest-Like Cells From Human Periodontal Ligament Cell-Derived Induced Pluripotent Stem
534 Cells. J Cell Physiol. 2017; 232: 402–416. https://doi.org/10.1002/jcp.25437 PMID:
535 27206577
536 38. Michael D, Wagoner MD, Bohrer LR, Aldrich BT, Greiner MA, Mullins RF et al.
537 Feeder-free differentiation of cells exhibiting characteristics of corneal endothelium from
538 human induced pluripotent stem cells. Biol Open. 2018; 7: 5.
539 http://dx.doi.org/10.1242/bio.032102 PMID: 29685994

bioRxiv preprint doi: https://doi.org/10.1101/432302; this version posted October 1, 2018. The copyright holder for this preprint (which was not certified by peer review) is the author/funder, who has granted bioRxiv a license to display the preprint in perpetuity. It is made available under aCC-BY 4.0 International license.

39. Bajpai R, Chen DA, Rada-Iglesias A, Zhang J, Xiong Y, Helms J et al. CHD7 cooperates with PBAF to control multipotent neural crest formation. Nature. 2010; 463: 958–962. https://doi.org/10.1038/nature08733 PMID: 20130577

40. Gallego RI, Pai AA, Tung J, Gilad Y. RNA-seq: impact of RNA degradation on transcript quantification. BMC Biol. 2014; 12: 42. https://dx.doi.org/10.1186%2F1741-7007-12-42 PMID: 24885439

41. Wang Z, Gerstein M, Snyder M. RNA-Seq: a revolutionary tool for transcriptomics. Nat Rev Genet. 2009; 10: 57–63. https://doi.org/10.1038/nrg2484 PMID: 19015660

42. Mortazavi A, Williams BA, McCue K, Schaeffer L, Wold B. Mapping and quantifying mammalian transcriptomes by RNA-Seq. Nat Methods. 2008; 5: 621–628. https://doi.org/10.1038/nmeth.1226 PMID: 18516045

43. Sauka-Spengler T, Meulemans D, Jones M, Bronner-Fraser M. Ancient evolutionary origin of the neural crest gene regulatory network. Dev Cell. 2007; 13: 405–420. https://doi.org/10.1016/j.devcel.2007.08.005 PMID: 17765683

44. Nikitina N, Sauka-Spengler T, Bronner-Fraser M. Dissecting early regulatory relationships in the lamprey neural crest gene network. Proc Natl Acad Sci U S A. 2008; 105: 20083 20088. https://dx.doi.org/10.1073%2Fpnas.0806009105 PMID: 19104059

bioRxiv preprint doi: https://doi.org/10.1101/432302; this version posted October 1, 2018. The copyright holder for this preprint (which was not certified by peer review) is the author/funder, who has granted bioRxiv a license to display the preprint in perpetuity. It is made available under aCC-BY 4.0 International license.

558 45. Khudyakov J, Bronner-Fraser M. Comprehensive spatiotemporal analysis of early chick
559 neural crest network genes. Dev Dyn. 2009; 238: 716–723.
560 https://doi.org/10.1002/dvdy.21881 PMID: 19235729
561 46. Hill RE, Jones PF, Rees AR, Sime CM, Justice MJ, Copeland NG et al. A new family of
562 mouse homeo box-containing genes: molecular structure, chromosomal location, and
563 developmental expression of Hox-7.1. Genes Dev. 1989; 3: 26–37. PMID: 2565278
564 47. Suzuki A, Ueno N, Hemmati-Brivanlou A. Xenopus msx1 mediates epidermal induction
565 and
566 neural inhibition by BMP4. Development. 1997; 124: 3037–3044. PMID: 9272945
567 48. Simões-Costa M, McKeown SJ, Tan-Cabugao J, Sauka-Spengler T, Bronner ME. Dynamic
568 and differential regulation of stem cell factor FoxD3 in the neural crest is Encrypted in the
569 genome. PLoS Genet. 2012; 8: e1003142. https://doi.org/10.1371/journal.pgen.1003142
570 PMID: 23284303
571 49. Goulding MD, Chalepakis G, Deutsch U, Erselius JR, Gruss P. Pax-3, a novel murine DNA
572 binding protein expressed during early neurogenesis. EMBO J. 1991; 10: 1135–1147.
573 PMID: 202218
574 50. Bang AG, Papalopulu N, Goulding MD, Kintner C. Expression of Pax-3 in the lateral neural
575 plate is dependent on a Wnt- mediated signal from posterior nonaxial mesoderm. Dev Biol.

bioRxiv preprint doi: https://doi.org/10.1101/432302; this version posted October 1, 2018. The copyright holder for this preprint (which was not certified by peer review) is the author/funder, who has granted bioRxiv a license to display the preprint in perpetuity. It is made available under aCC-BY 4.0 International license.

1991; 212: 366–380. https://doi.org/10.1006/dbio.1999.9319 PMID: 10433827

51. Alkobtawi M, Ray H, Barriga EH, Moreno M, Kerney R, Monsoro-Burq AH et al. Characterization of Pax3 and Sox10 transgenic Xenopus laevis embryos as tools to study neural crest development. Dev Biol. 2018; 17: https://doi.org/10.1016/j.ydbio.2018.02.020 PMID: 29522707

52. Maczkowiak F, Matéos S, Wang E, Roche D, Harland R, Monsoro-Burq AH. The Pax3 and Pax7 paralogs cooperate in neural and neural crest patterning using distinct molecular mechanisms, in Xenopus laevis embryos. Dev Biol. 2010; 340: 381–396. https://doi.org/10.1016/j.ydbio.2010.01.022 PMID: 20116373

53. Krishnakumar R, Chen AF, Pantovich MG, Danial M, Parchem RJ, Labosky PA et al. FOXD3 Regulates Pluripotent Stem Cell Potential by Simultaneously Initiating and Repressing Enhancer Activity. Cell Stem Cell. 2016; 18: 104–117. https://doi.org/10.1016/j.stem.2015.10.003 PMID: 26748757

54. Desanlis I, Felstead HL, Edwards DR, Wheeler GN. ADAMTS9, a member of the ADAMTS family, in Xenopus development. Gene Expr Patterns. 2018; 29: 72–81. https://doi.org/10.1016/j.gep.2018.06.001 PMID: 29935379

55. Porter S, Clark IM, Kevorkian L, Edwards DR. The ADAMTS metalloproteinases. Biochem J. 2005; 386: 15–27. https://doi.org/10.1042/BJ20040424 PMID: 15554875

bioRxiv preprint doi: https://doi.org/10.1101/432302; this version posted October 1, 2018. The copyright holder for this preprint (which was not certified by peer review) is the author/funder, who has granted bioRxiv a license to display the preprint in perpetuity. It is made available under aCC-BY 4.0 International license.

594 56. Hubmacher D, Apte SS. ADAMTS proteins as modulators of microfibril formation and
595 function. Matrix Biol. 2015; 47: 34–43. https://doi.org/10.1016/j.matbio.2015.05.004
596 PMID: 25957949
597 57. Chen WV, Maniatis T. Clustered protocadherins. Development. 2013; 140: 3297–302.
598 https://doi.org/10.1242/dev.090621 PMID: 23900538
599 58. Okita K, Ichisaka T, Yamanaka S. Generation of germline competent induced pluripotent
600 stem cells. Nature. 2007; 448: 313–317. https://doi.org/10.1038/nature05934
601 PMID: 17554338
602 59. Ishii M, Arias AC, Liu L, Chen YB, Bronner ME, Maxson RE. A stable cranial neural crest
603 cell line from mouse. Stem Cells Dev. 2012; 21: 3069–3080.
604 https://doi.org/10.1089/scd.2012.0155 PMID: 22889333
605 60. Antonellis A, Bennett WR, Menheniott TR, Prasad AB, Lee-Lin SQ; NISC Comparative
606 Sequencing Program et al. Deletion of long-range sequences at Sox10 compromises
607 developmental expression in a mouse model of Waardenburg-Shah (WS4) syndrome. Hum
608 Mol Genet. 2006; 15: 259–271. https://doi.org/10.1093/hmg/ddi442 PMID: 16330480
609 61. Betancur P, Bronner-Fraser M, Sauka-Spengler T. Genomic code for Sox10 activation
610 reveals a key regulatory enhancer for cranial neural crest. Proc Natl Acad Sci U S A. 2010;
611 107: 3570–3575. https://doi.org/10.1073/pnas.0906596107 PMID: 20139305

bioRxiv preprint doi: https://doi.org/10.1101/432302; this version posted October 1, 2018. The copyright holder for this preprint (which was not certified by peer review) is the author/funder, who has granted bioRxiv a license to display the preprint in perpetuity. It is made available under aCC-BY 4.0 International license.

612 62. Rinon A, Molchadsky A, Nathan E, Yovel G, Rotter V, Sarig R et al. p53 coordinates
613 cranial neural crest cell growth and epithelial-mesenchymal transition/delamination
614 processes. Development. 2011; 138: 1827–1838. https://doi.org/10.1242/dev.053645
615 PMID: 21447558
616 63. Hari L, Miescher I, Shakhova O, Suter U, Chin L, Taketo M et al. Temporal control
617 of neural crest lineage generation by Wnt/β- catenin signaling. Development. 2012; 139:
618 2107–2117. https://doi.org/10.1242/dev.073064 PMID: 22573620
619 64. Murko C, Bronner ME. Tissue specific regulation of the chick Sox10E1 enhancer by
620 different Sox family members. Dev Biol. 2016; 422: 47–57.
621 https://doi.org/10.1016/j.ydbio.2016.12.004 PMID: 28012818
622 65. Spokony RF, Aoki Y, Saint-Germain N, Magner-Fink E, Saint-Jeannet JP. The transcription
623 factor Sox9 is required for cranial neural crest development in Xenopus. Development.
624 2002; 129: 421–432. PMID: 11807034
625 66. Perez-Alcala S, Nieto MA, Barbas JA. LSox5 regulates RhoB expression in the neural tube
626 and promotes generation of the neural crest. Development. 2004; 131: 4455–4465.
627 https://doi.org/10.1242/dev.01329 PMID: 15306568
628 67. Barembaum M, Bronner ME. Identification and dissection of a key enhancer mediating
629 cranial neural crest specific expression of transcription factor, Ets-1. Dev Biol. 2013; 382:

bioRxiv preprint doi: https://doi.org/10.1101/432302; this version posted October 1, 2018. The copyright holder for this preprint (which was not certified by peer review) is the author/funder, who has granted bioRxiv a license to display the preprint in perpetuity. It is made available under aCC-BY 4.0 International license.

567-575. https://dx.doi.org/10.1016%2Fj.ydbio.2013.08.009 PMID: 23969311

68. Nagai T, Aruga J, Takada S, Günther T, Spörle R, Schughart K et al. The expression of the mouse Zic1, Zic2, and Zic3 gene suggests an essential role for Zic genes in body pattern formation. Dev Biol. 1997; 182: 299–313. https://doi.org/10.1006/dbio.1996.8449 PMID: 9070329

69. Teslaa JJ, Keller AN, Nyholm MK, Grinblat Y. Zebrafish Zic2a and Zic2b regulate neural crest and craniofacial development. Dev Biol. 2013; 380: 73–86. https://doi.org/10.1016/j.ydbio.2013.04.033 PMID: 23665173

70. Das A, Crump JG. Bmps and id2a act upstream of Twist1 to restrict ectomesenchyme potential of the cranial neural crest. PLoS Genet.2012; 8: e1002710. https://doi.org/10.1371/journal.pgen.1002710 PMID: 22589745

71. Machon O, Masek J, Machonova O, Krauss S, Kozmik Z. Meis2 is essential for cranial and cardiac neural crest development. BMC Dev Biol. 2015;15. https://doi.org/10.1186/s12861-015-0093-6 PMID: 26545946

72. Mitchell PJ, Timmons PM, Hébert JM, Rigby PW, Tjian R. Transcription factor AP-2 is expressed in neural crest cell lineages during mouse embryogenesis. Genes Dev. 1991; 5: 105–119. PMID: 1989904

73. Shen H, Wilke T, Ashique AM, Narvey M, Zerucha T, Savino E. Chicken transcription

bioRxiv preprint doi: https://doi.org/10.1101/432302; this version posted October 1, 2018. The copyright holder for this preprint (which was not certified by peer review) is the author/funder, who has granted bioRxiv a license to display the preprint in perpetuity. It is made available under aCC-BY 4.0 International license.

factor AP-2: cloning, expression and its role in outgrowth of facialprominences and limb buds. Dev Biol. 1997; 188: 248–266. https://doi.org/10.1006/dbio.1997.8617 PMID: 9268573

74. Luo T, Lee YH, Saint-Jeannet JP, Sargent TD. Induction of neural crest in Xenopus by transcription factor AP2alpha. Proc Natl Acad Sci U S A. 2003; 100: 532–537. https://doi.org/10.1073/pnas.0237226100 PMID: 12511599

75. de Crozé N, Maczkowiak F, Monsoro-Burq AH. Reiterative AP2a activity controls sequential steps in the neural crest gene regulatory network. Proc Natl Acad Sci U S A. 2011; 108: 155–160. https://dx.doi.org/10.1073%2Fpnas.1010740107 PMID: 21169220

76. Wang WD, Melville DB, Montero-Balaguer M, Hatzopoulos AK, Knapik EW. Tfap2a and Foxd3 regulate early steps in the development of the neural crest progenitor population. Dev Biol. 2011; 360: 173–185. https://doi.org/10.1016/j.ydbio.2011.09.019 PMID: 21963426

77. Powell DR, Hernandez-Lagunas L, LaMonica K, Artinger KB. Prdm1a directly activates foxd3 and tfap2a during zebrafish neural crest specification. Development. 2013; 140: 3445–3455. https://doi.org/10.1242/dev.096164 PMID: 23900542

78. Yang L, Zhang H, Hu G, Wang H, Abate-Shen C, Shen MM. An early phase of embryonic Dlx5 expression defines the rostral boundary of the neural plate. J Neurosci. 1998; 18:

bioRxiv preprint doi: https://doi.org/10.1101/432302; this version posted October 1, 2018. The copyright holder for this preprint (which was not certified by peer review) is the author/funder, who has granted bioRxiv a license to display the preprint in perpetuity. It is made available under aCC-BY 4.0 International license.

8322–8330. PMID: 9763476

79. Luo T, Matsuo-Takasaki M, Lim JH, Sargent TD. Differential regulation of Dlx gene expression by a BMP morphogenetic gradient. Int J Dev Biol. 2001; 45: 681–684. PMID:11461005

80. Li B, Kuriyama S, Moreno M, Mayor R. The posteriorizing gene Gbx2 is a direct target of Wnt signalling and the earliest factor in neural crest induction. Development. 2009; 136: 3267–3278. https://doi.org/10.1242/dev.036954 PMID: 19736322

81. Nakata K, Nagai T, Aruga J, Mikoshiba K. Xenopus Zic family and its role in neural crest development. Mech Dev. 1998; 75: 43–51. https://doi.org/10.1016/S0925-4773(98)00073 PMID: 9739105

82. Dottori M, Gross MK, Labosky P, Goulding M. The winged helix transcription factor Foxd3 suppresses interneuron differentiation and promotes neural crest cell fate. Development. 2001; 128: 4127–4138. PMID: 11684651

83. Kos R, Reedy MV, Johnson RL, Erickson CA. The winged-helix transcription factor FoxD3 is important for establishing the neural crest lineage and repressing melanogenesis in avian embryos. Development. 2001; 128: 1467–1479. PMID: 11262245

84. Wilson YM, Richards KL, Ford-Perriss ML, Panthier JJ, Murphy M. Neural crest cell lineage segregation in the mouse neural tube. Development. 2004; 131: 6153–6162.

bioRxiv preprint doi: https://doi.org/10.1101/432302; this version posted October 1, 2018. The copyright holder for this preprint (which was not certified by peer review) is the author/funder, who has granted bioRxiv a license to display the preprint in perpetuity. It is made available under aCC-BY 4.0 International license.

https://doi.org/10.1242/dev.01533 PMID: 15548576

85. Liu L, Chong SW, Balasubramaniyan NV, Korzh V, Ge R. Platelet-derived growth factor receptor alpha (pdgfr-α) gene in zebrafish embryonic development. Mech Dev. 2002; 116: 227–230. https://doi.org/10.1016/S0925-4773(02)00142-9 PMID: 12128230

86. Liu KJ, Harland RM. Cloning and characterization of Xenopus Id4 reveals differing roles for Id genes. Dev Biol. 2003; 264: 339–351. https://doi.org/10.1016/j.ydbio.2003.08.017 PMID: 14651922

87. Figueiredo AL, Maczkowiak F, Borday C, Pla P, Sittewelle M, Pegoraro C et al. PFKFB4 control of AKT signaling is essential for premigratory and migratory neural crest formation. Development. 2017; 144: 4183–4194. https://doi.org/10.1242/dev.157644 PMID: 29038306

88. Yang X, Li J, Zeng W, Li C, Mao B. Elongator Protein 3 (Elp3) stabilizes Snail1 and regulates neural crest migration in Xenopus. Sci Rep. 2016; 6: 26238. https://doi.org/10.1038/srep26238 PMID: 27189455

89. Sefton M, Sánchez S, Nieto MA. Conserved and divergent roles for members of the Snail family of transcription factors in the chick and mouse embryo. Development. 1998; 125: 3111–3121. PMID: 9671584

90. del Barrio MG, Nieto MA. Overexpression of Snail family members highlights their ability to promote chick neural crest formation. Development. 2002; 129: 1583–1593. PMID:

bioRxiv preprint doi: https://doi.org/10.1101/432302; this version posted October 1, 2018. The copyright holder for this preprint (which was not certified by peer review) is the author/funder, who has granted bioRxiv a license to display the preprint in perpetuity. It is made available under aCC-BY 4.0 International license.

11923196

91. Aybar MJ, Nieto MA, Mayor R. Snail precedes Slug in the genetic cascade required for the specification and migration of the Xenopus neural crest. Development. 2003; 130: 483–494. http://doi.org/10.1242/dev.00238 PMID: 12490555

92. Nieto MA, Sargent MG, Wilkinson DG, Cooke J. Control of cell behavior during vertebrate development by Slug, a zinc finger gene. Science. 1994; 264: 835–859. http://doi.org/10.1126/science.7513443 PMID: 7513443

93. Jiang R, Lan Y, Norton CR, Sundberg JP, Gridley T. The Slug gene is not essential for mesoderm or neural crest development in mice. Dev Biol. 1998; 198: 277–285. https://doi.org/10.1016/S0012-1606(98)80005-5 PMID: 9659933

94. Tien CL, Jones A, Wang H, Gerigk M, Nozell S, Chang C. Snail2/Slug cooperates with Polycomb repressive complex 2 (PRC2) to regulate neural crest development. Development. 2015; 142: 722–731. https://doi.org/10.1242/dev.111997 PMID: 25617436

95. Martin BL, Harland PM. Hypaxial muscle migration during primary myogenesis in Xenopus laevis. Dev Biol. 2001; 239: 270–280. https://doi.org/10.1006/dbio.2001.0434 PMID: 11784034

96. Cheung M, Briscoe J. Neural crest development is regulated by the transcription factor Sox9. Development. 2003; 130: 5681–5693. https://doi.org/10.1242/dev.00808 PMID:

bioRxiv preprint doi: https://doi.org/10.1101/432302; this version posted October 1, 2018. The copyright holder for this preprint (which was not certified by peer review) is the author/funder, who has granted bioRxiv a license to display the preprint in perpetuity. It is made available under aCC-BY 4.0 International license.

14522876

97. Cheung M, Chaboissier MC, Mynett A, Hirst E, Schedl A, Briscoe J. The transcriptional control of trunk neural crest induction, survival, and delamination. Dev Cell. 2005; 8: 179–192. https://doi.org/10.1016/j.devcel.2004.12.010 PMID: 15691760

98. Honoré SM, Aybar MJ, Mayor R. Sox10 is required for the early development of the prospective neural crest in Xenopus embryos. Dev Biol. 2003; 260: 79–96. https://doi.org/10.1016/S0012-1606(03)00247-1 PMID: 12885557

99. McKeown SJ, Lee VM, Bronner-Fraser M, Newgreen DF, Farlie PG. Sox10 overexpression induces neural crest-like cells from all dorsoventral levels of the neural tube but inhibits differentiation. Dev Dyn. 2005; 233: 430–444. https://doi.org/10.1002/dvdy.20341 PMID: 15768395

100. Prasad MK, Reed X, Gorkin DU, Cronin JC, McAdow AR, Chain K et al. SOX10 directly modulates ERBB3 transcription via an intronic neural crest enhancer. BMC Dev Biol. 2011; 11. https://doi.org/10.1186/1471-213X-11-40 PMID: 21672228

101. Baggiolini A, Varum S, Mateos JM, Bettosini D, John N, Bonalli M et al. Premigratory and migratory neural crest cells are multipotent in vivo. Cell Stem Cell. 2015; 16: 314–322. https://doi.org/10.1016/j.stem.2015.02.017 PMID: 25748934

bioRxiv preprint doi: https://doi.org/10.1101/432302; this version posted October 1, 2018. The copyright holder for this preprint (which was not certified by peer review) is the author/funder, who has granted bioRxiv a license to display the preprint in perpetuity. It is made available under aCC-BY 4.0 International license.

738 102. McKinney MC, McLennan R, Kulesa PM. Angiopoietin 2 signaling plays a critical role in
739 neural crest cell migration. BMC Biol. 2016; 14. https://doi.org/10.1186/s12915-016-0323-
740 9 PMID: 27978830
741 103. Lee HO, Levorse JM, Shin MK. The endothelin receptor-B is required for the migration of
742 neural crest-derived melanocyte and enteric neuron precursors. Dev Biol. 2003; 259: 162
743 175. https://doi.org/10.1016/S0012-1606(03)00160-X PMID: 12812796
744 104. Giovannone D, Ortega B, Reyes M, El-Ghali N, Rabadi M, Sao S et al. Chicken trunk
745 neural crest migration visualized with HNK1. Acta Histochem. 2015; 117: 255–266.
746 https://doi.org/10.1016/j.acthis.2015.03.002 PMID: 25805416
747 105. Zuhdi N, Ortega B, Giovannone D, Ra H, Reyes M, Asención V et al. Slits Affect the
748 Timely Migration of Neural Crest Cells Via Robo Receptor. Dev Dyn. 2012; 241: 1274
749 1288. https://dx.doi.org/10.1002%2Fdvdy.23817 PMID: 22689303
750 106. Chiovaro F, Chiquet-Ehrismann R, Chiquet M. Transcriptional regulation of tenascin
751 genes. Cell Adh Migr. 2015; 9: 34–47.
752 https://dx.doi.org/10.1080%2F19336918.2015.1008333 PMID: 25793574
753 107. Taneyhill AL, Coles EG, Bronner-Fraser M. Snail2 directly represses cadherin6B during
754 epithelial-to-mesenchymal transitions of the neural crest. Development. 2007; 134: 1480–
755 1490. https://dx.doi.org/10.1242%2Fdev.02834 PMID: 17344227

bioRxiv preprint doi: https://doi.org/10.1101/432302; this version posted October 1, 2018. The copyright holder for this preprint (which was not certified by peer review) is the author/funder, who has granted bioRxiv a license to display the preprint in perpetuity. It is made available under aCC-BY 4.0 International license.

756 108. Groysman M, Shoval I, Kalcheim C. A negative modulatory role for rho and rho-
757 associated
758 kinase signaling in delamination of neural crest cells. Neural Develop. 2008; 3: 27.
759 https://dx.doi.org/10.1186%2F1749-8104-3-27 PMID: 18945340
760 109. Vega FM, Thomas M, Reymond N, Ridley AJ. The Rho GTPase RhoB regulates cadherin
761 expression and epithelial cell-cell interaction. Cell Commun Signal. 2015; 13: 6.
762 https://doi.org/10.1186/s12964-015-0085-y PMID: 25630770
763 110. Liu Q, Dalman MR, Sarmah S, Chen S, Chen Y, Hurlbut AK et al. Cell adhesion molecule
764 cadherin-6 function in zebrafish cranial and lateral line ganglia development. Dev Dyn.
765 2011; 240: 1716–26. https://doi.org/10.1002/dvdy.22665 PMID: 21584906
766 111. Chiovaro F, Chiquet-Ehrismann R, Chiquet M. Transcriptional regulation of tenascin
767 genes. Cell Adh Migr. 2015; 9: 34–47.
768 https://dx.doi.org/10.1080%2F19336918.2015.1008333 PMID: 25793574
769 112. Tomczuk M, Takahashi Y, Huang J, Murase S, Mistretta M, Klaffky E et al. Role of
770 multiple beta1 integrins in cell adhesion to the disintegrin domains of ADAMs 2 and 3.
771 Exp Cell Res. 2003; 290: 68–81. https://doi.org/10.1016/S0014-4827(03)00307-0 PMID:
772 14516789
773 113. Dennis AR, McLennan R, Jessica MT, Craig LS, Jeffrey SH, Kulesa PM. The neural

bioRxiv preprint doi: https://doi.org/10.1101/432302; this version posted October 1, 2018. The copyright holder for this preprint (which was not certified by peer review) is the author/funder, who has granted bioRxiv a license to display the preprint in perpetuity. It is made available under aCC-BY 4.0 International license.

774 crest cell cycle is related to phases of migration in the head. Development. 2014; 141:

775 1095–1103. https://dx.doi.org/10.1242%2Fdev.098855 PMID: 24550117

bioRxiv preprint doi: https://doi.org/10.1101/432302; this version posted October 1, 2018. The copyright holder for this preprint (which was not certified by peer review) is the author/funder, who has granted bioRxiv a license to display the preprint in perpetuity. It is made available under aCC-BY 4.0 International license.

Fig.4.

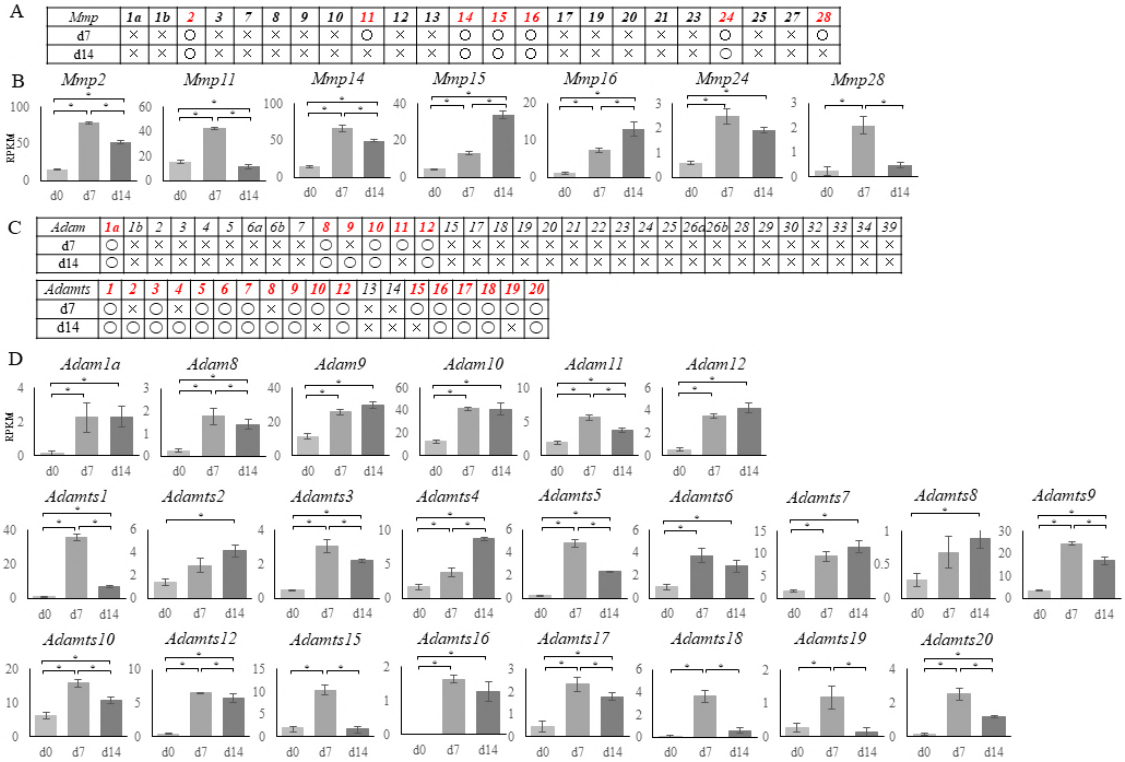

bioRxiv preprint doi: https://doi.org/10.1101/432302; this version posted October 1, 2018. The copyright holder for this preprint (which was not certified by peer review) is the author/funder, who has granted bioRxiv a license to display the preprint in perpetuity. It is made available under aCC-BY 4.0 International license.

Fig.2 .

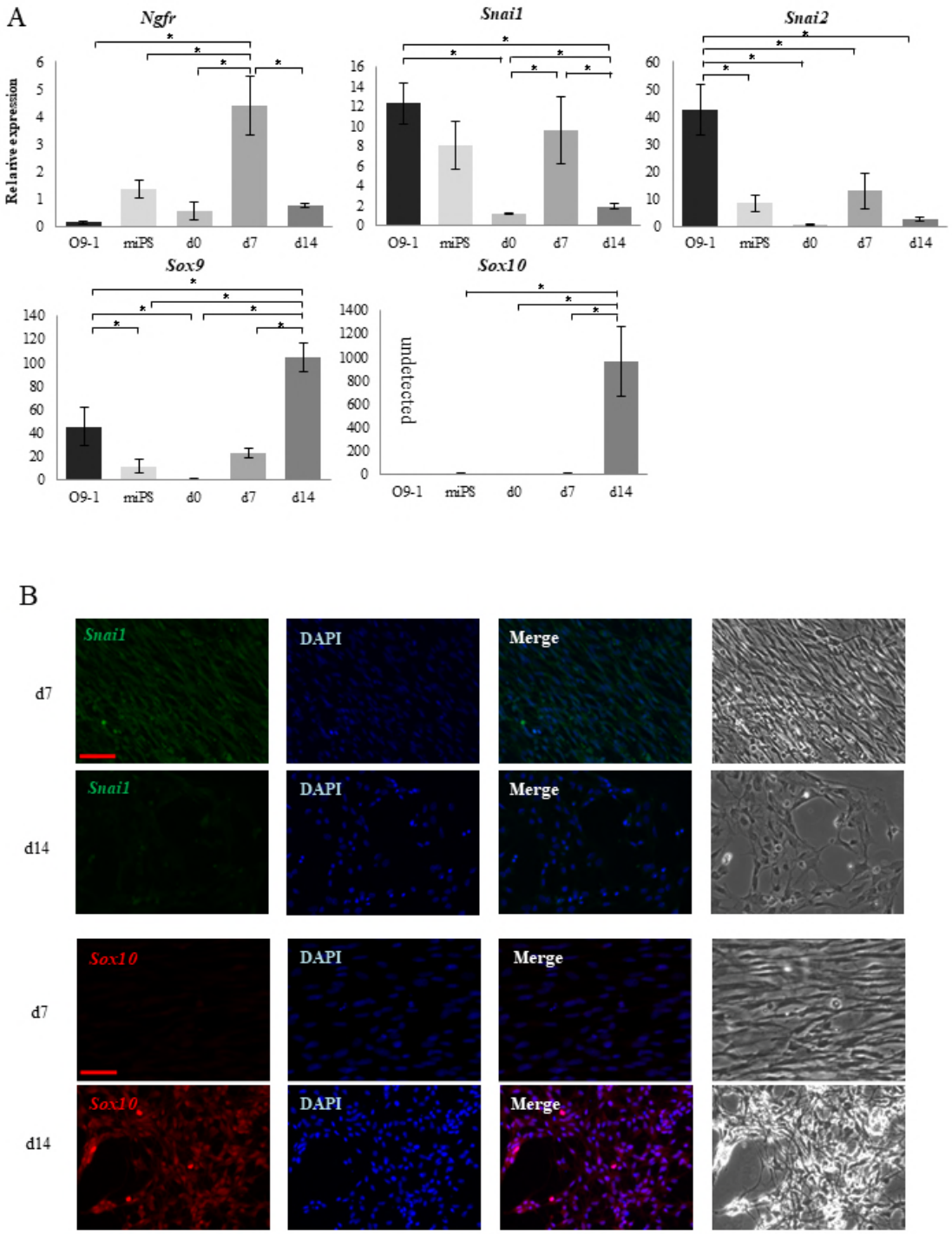

bioRxiv preprint doi: https://doi.org/10.1101/432302; this version posted October 1, 2018. The copyright holder for this preprint (which was not certified by peer review) is the author/funder, who has granted bioRxiv a license to display the preprint in perpetuity. It is made available under aCC-BY 4.0 International license.

Fig. 3.

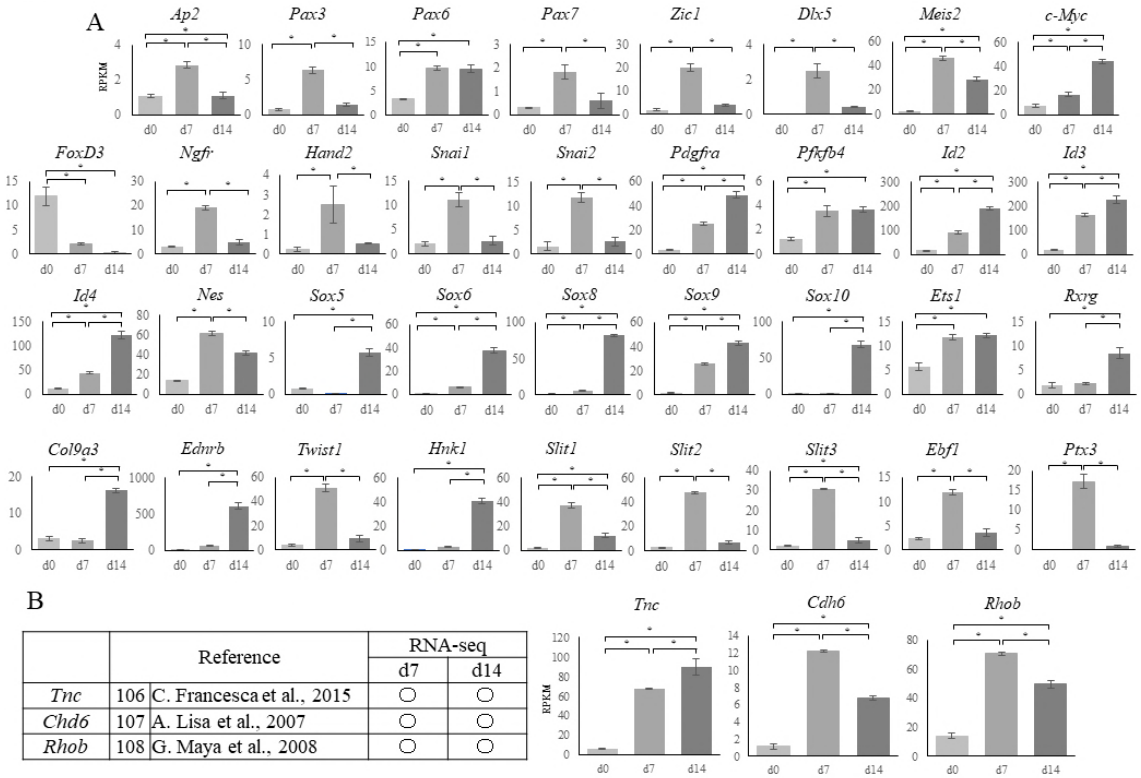

B

	Reference		RNA-seq	
			d7	d14
Tnc	106	C. Francesca et al., 2015	○	○
Chd6	107	A. Lisa et al., 2007	○	○
Rhob	108	G. Maya et al., 2008	○	○

bioRxiv preprint doi: https://doi.org/10.1101/432302; this version posted October 1, 2018. The copyright holder for this preprint (which was not certified by peer review) is the author/funder, who has granted bioRxiv a license to display the preprint in perpetuity. It is made available under aCC-BY 4.0 International license.

Fig 1